Kamal Prakash Pandey[1],

Rakesh Kumar Singh[2],

Surya Bhushan Dubey[3],

Amrees Pandey[4*]

High-Performance Multi-Band Dual-Port MIMO Antenna for Ku and K-Band Communication Systems

Abstract*:* - This paper presents a compact dual-port MIMO antenna, designed and optimized using full-wave HFSS simulations, for Ku- and K-band radar and satellite communication applications. The antenna employs a rectangular patch with integrated ring-slot stubs, enhancing bandwidth, gain, and port isolation. With overall dimensions of 24×24×1.6 mm³ on an FR-4 substrate, the simulated results demonstrate three wide impedance bands: 13.56–14.86 GHz, 16.60–18.76 GHz, and 20.50–28.36 GHz, effectively covering the Ku and K bands. The antenna achieves a peak simulated gain of 9.06 dBi, radiation efficiency above 85%, and inter-port isolation greater than 18 dB. Excellent diversity performance is observed, with an envelope correlation coefficient (ECC) below 0.012, diversity gain around 9.9 dB, and TARC under –10 dB. These simulation results confirm that the proposed design is a compact, high-performance, and reliable MIMO solution for next-generation radar, satellite, and vehicular communication systems operating in Ku and K bands.

Keywords*:* MIMO antenna, Ku/K-band, HFSS simulation, isolation, gain enhancement, ECC, satellite communication.

1. Introduction

The rapid advancement of wireless communication technologies has significantly increased the demand for high data rates, robust reliability, and multi-band operation in modern communication systems. To meet these requirements, Multiple-Input Multiple-Output (MIMO) technology has emerged as a pivotal enabler, offering improvements in spectral efficiency, link reliability, and system capacity without requiring additional bandwidth or transmission power [1]–[4]. By exploiting spatial diversity, MIMO systems can simultaneously transmit and receive multiple data streams, enhancing the overall data throughput and quality of service. These benefits are critical for contemporary applications, including fifth-generation (5G) networks, vehicular communication, satellite links, and radar systems [4, 9, 12, 26].

Despite its advantages, MIMO deployment faces several challenges, particularly for compact and multi-band devices. One of the major challenges is mutual coupling between closely spaced antenna elements, which can degrade performance by increasing the envelope correlation coefficient (ECC), reducing port isolation, and lowering diversity gain (DG), thus adversely affecting system throughput and reliability [5]–[7, 29]. The severity of mutual coupling increases as the inter-element spacing decreases, a common requirement in modern compact devices [18, 23, 29]. Consequently, MIMO antenna designs must minimize mutual coupling while ensuring wide impedance bandwidth, high gain, and low ECC for effective multi-port operation [8, 10, 16, 18]. Various strategies have been investigated to mitigate mutual coupling in MIMO antennas. Techniques such as defected ground structures (DGS), metamaterials, parasitic elements, neutralization lines, and optimized element spacing have been employed to enhance isolation and improve MIMO performance [10, 16, 18, 23, 29]. These methods are

[1]Department of Electronics and Communication Engineering, BBS College of Engineering and Technology, Prayagraj, Uttar Pradesh, India
[2, 4]Department of Electronics and Communication Engineering, Shambhunath Institute of Engineering and Technology (SIET), Prayagraj, Uttar Pradesh, India
[3]Department of Electrical and Electronics Engineering, S. R. Institute of Management and Technology, Lucknow, Uttar Pradesh, India
pandeykamal.1976@gmail.com1, rksingh_rakesh@yahoo.com2, suryadubey1@gmail.com3, amrishpandey19@gmail.com4
*Corresponding Author Email: amrishpandey19@gmail.com

particularly important for antennas operating at Ku (12–18 GHz) and K (18–27 GHz) bands, where high-frequency propagation is sensitive to surface waves, fabrication tolerances, and mutual coupling effects [25]–[27, 31]–[34]. The development of dual- and multi-band MIMO antennas has become increasingly essential for modern communication systems. Multi-band operation reduces reliance on multiple single-band antennas, thereby minimizing system complexity, lowering device footprint, and improving cost-effectiveness [8]–[11, 24, 25, 31]. Dual-band designs are especially relevant for satellite and radar systems, which require simultaneous coverage of multiple frequency bands to support diverse applications such as high-resolution imaging, remote sensing, and secure communication [25, 26, 35]–[37]. Design approaches such as slot-loading, parasitic elements, and ring-shaped stubs have been implemented to enhance impedance bandwidth, gain, and port isolation in multi-band MIMO antennas [15, 26, 27, 30, 36]. These techniques enable the realization of compact, high-performance antennas suitable for demanding modern communication systems.

Performance metrics such as ECC, DG, and Total Active Reflection Coefficient (TARC) are critical in evaluating MIMO antennas. ECC quantifies the correlation between antenna ports, with lower values indicating improved spatial diversity and minimal interference between elements [12]–[14, 20, 38]. DG measures the improvement in signal reliability achievable through multiple antennas without increasing transmit power [17, 38]. TARC evaluates the overall reflection behavior under multi-port excitation, indicating how efficiently an antenna handles multi-port operation with minimal power reflection [17, 39]. Collectively, these metrics provide a comprehensive framework for assessing high-performance MIMO antennas, particularly for multi-band and high-frequency applications [12]–[14, 17, 20, 38]–[40].

Recent literature demonstrates various approaches to designing compact MIMO antennas for Ku- and K-band applications. For instance, Addepalli and Anitha [25] proposed a two-port MIMO antenna with parasitic reflectors, achieving wideband operation and high isolation across UWB, X-, and Ku-band frequencies. Dwivedi et al. [26] developed a quad-port circularly polarized dielectric resonator MIMO antenna with beam-tilting capability for vehicular communications. Tan and Tripathy [27] presented a miniaturized T-shaped MIMO antenna for X- and Ku-band operation with enhanced radiation efficiency. Other studies explored DGS-based multi-band MIMO antennas [18, 28], metasurface-inspired designs [16, 23], graphene-based radiators [7], and UWB structures [17, 19, 30, 31]. Advanced designs have also investigated multi-port pattern diversity [19], Franklin array-based 5G antennas [31], and 3D-printed compact MIMO arrays [24, 32]. Despite these efforts, many designs are either large, offer moderate isolation, or exhibit suboptimal ECC, highlighting the need for more compact and high-performance multi-band MIMO solutions [21]–[24, 33]–[40].

Existing literature emphasizes the inherent trade-offs in MIMO antenna design between compactness, bandwidth, gain, and mutual coupling. While significant advancements have been made, achieving a compact antenna with high gain, wide multi-band operation, low ECC, strong isolation, and high radiation efficiency remains challenging [21]–[27, 29, 30, 33]–[40]. This gap motivates the development of novel MIMO antennas optimized for Ku- and K-band operation, particularly for applications in radar, satellite communication, and vehicular systems.

In this context, the present work proposes a compact dual-port MIMO antenna with dimensions of $24\times24\times1.6$ mm³, designed to address challenges of inter-element coupling and multi-band operation. The antenna comprises two identical radiating elements arranged in parallel to maximize isolation, integrated with ring-slot stubs to enhance gain and bandwidth. The proposed design achieves port isolation >18 dB, ECC <0.012, and radiation efficiency >85%, ensuring excellent MIMO performance across Ku and K bands. By providing a compact form factor, wide impedance bandwidth, and superior diversity performance, the antenna represents a promising solution for next-generation radar, satellite communication, and vehicular communication systems [1]–[40].

2. Design Structure and Development of the Proposed MIMO Antenna

The proposed dual-port MIMO antenna is designed on an FR4 epoxy substrate with relative permittivity $\varepsilon_r = 4.4$, loss tangent $\tan\delta = 0.02$, and thickness 1.6 mm. The overall antenna dimensions are $24\times24\times1.6\text{mm}^3$, with a 50 Ω microstrip feed line. The top layer (radiating elements) is shown in green, and the bottom layer (ground plane) is yellow (Figure 1). The proposed design features dual-defected radiating patches with ring-slot loading, systematically optimized to enhance gain, bandwidth, and MIMO performance. The antenna evolution is carried out in four steps, as illustrated in Figure 2 and summarized in Table 1.

The proposed MIMO antenna was developed through a systematic four-step process, with each modification progressively enhancing its performance. In Step-1 (Antenna-1), two identical rectangular patches form the basic MIMO structure, providing the fundamental resonance. However, the bandwidth and gain are limited, port isolation is moderate, and ECC is relatively high, indicating significant correlation between the ports. In Step-2 (Antenna-2), parallel slots (8×6 mm²) are etched into the patches, improving impedance matching, slightly increasing bandwidth and gain, and achieving a more uniform current distribution that reduces minor mutual coupling.

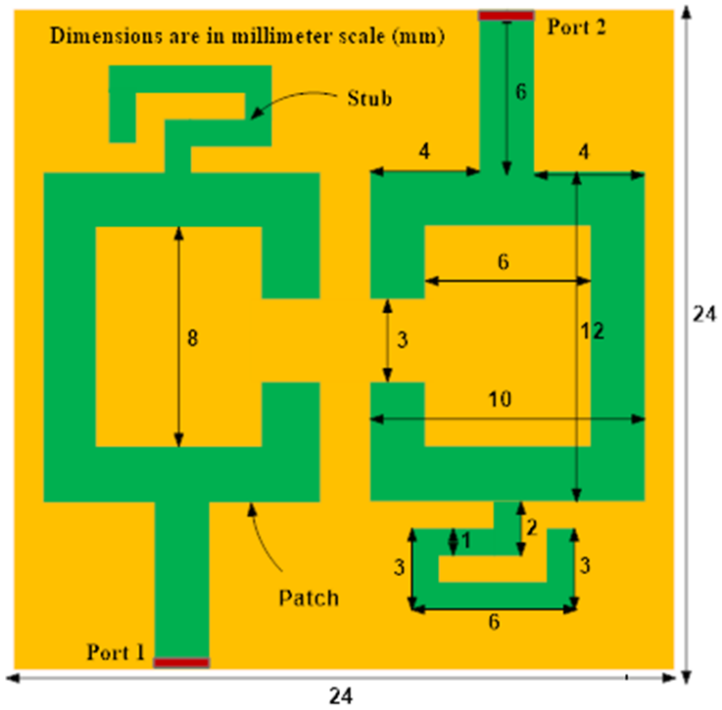

Fig. 1. Layout of the proposed dual-port MIMO antenna showing the radiating elements (green) on the top layer and the ground plane (yellow) on the bottom layer.

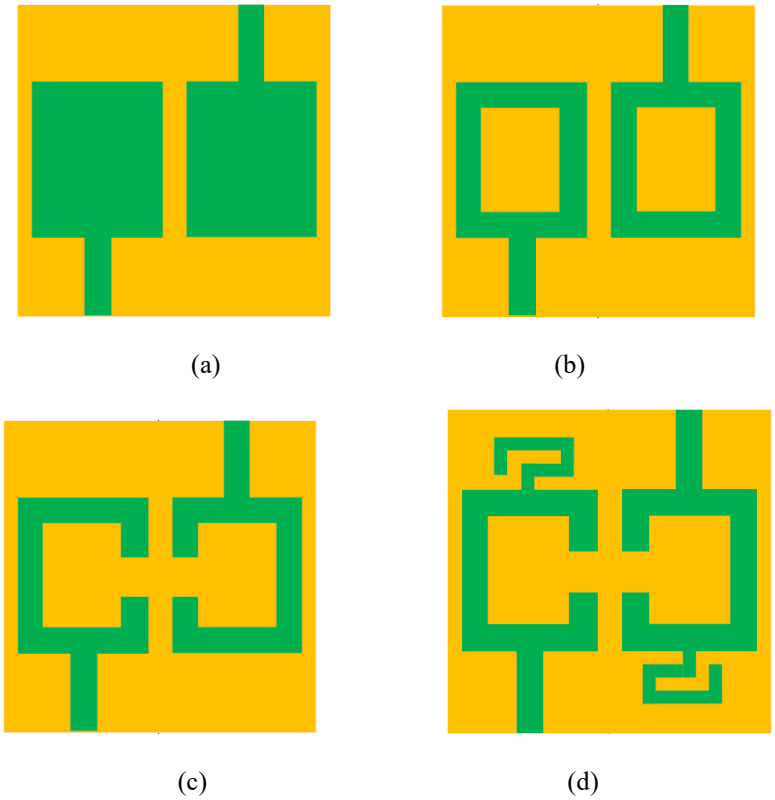

Fig. 2. Step-wise development of the proposed MIMO antenna: (a) Step-1: basic rectangular patches; (b) Step-2: parallel slots etched in patches; (c) Step-3: additional smaller slots; (d) Step-4: ring-shaped stub added, showing the final optimized design.

Table 1: Step-wise development of the proposed MIMO antenna

Step	Antenna	Radiating Element Modification	Feature Added	Effect on Performance
1	Antenna-1	Two identical rectangular patches (10×12 mm²)	Basic patch design	Establishes fundamental resonance
2	Antenna-2	Etched parallel rectangular slots (8×6 mm²) in patches	Slot-loading	Improved impedance matching & bandwidth
3	Antenna-3	Additional smaller slots (2×3 mm²) at right side of patches	Fine tuning of current distribution	Enhanced radiation characteristics, reduced unwanted coupling
4	Antenna-4 (Proposed)	Ring-shaped stub added on top of patches	Ring-slot loading	Maximized gain & bandwidth; optimized current flow for better MIMO performance

Step-3 (Antenna-3) introduces additional smaller slots (2×3 mm²) at the right side of the patches, refining current paths, further enhancing gain and bandwidth, and improving port isolation. ECC reduces at this stage, reflecting improved MIMO diversity performance. Finally, in Step-4 (Antenna-4, the proposed design), the addition of a ring-shaped stub introduces an extra resonance that maximizes gain and bandwidth. HFSS simulations confirm optimized port isolation, low ECC, high diversity gains (DG), and minimal total active reflection coefficient (TARC), demonstrating excellent MIMO performance. Overall, the Step-wise Development Table clearly illustrates the cause-effect relationship between structural modifications and performance improvements. Each design step from simple rectangular patches to ring-slot loaded patches with optimized spacing progressively enhances gain, bandwidth, isolation, and MIMO metrics. The carefully optimized 2 mm separation between patches minimizes mutual coupling without altering the basic patch shape. This systematic design approach validates that the proposed antenna achieves high-performance MIMO characteristics suitable for practical applications.

3. Results and Discussion

The proposed dual-port MIMO antenna was simulated using HFSS, and its performance was evaluated through multiple metrics, including return loss (S11, S22), mutual coupling (S12, S21), radiation efficiency, gain, envelope correlation coefficient (ECC), diversity gain (DG), total active reflection coefficient (TARC), and far-field radiation patterns.

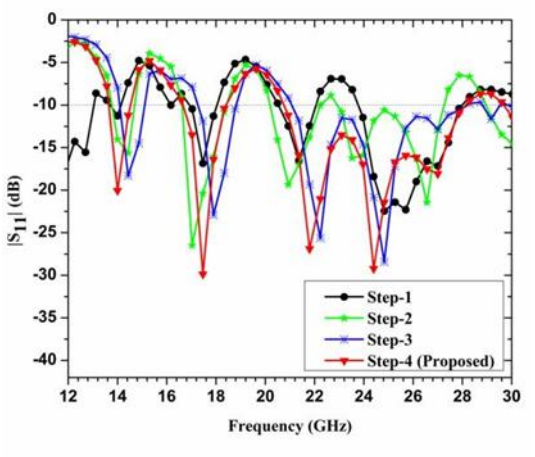

(a)

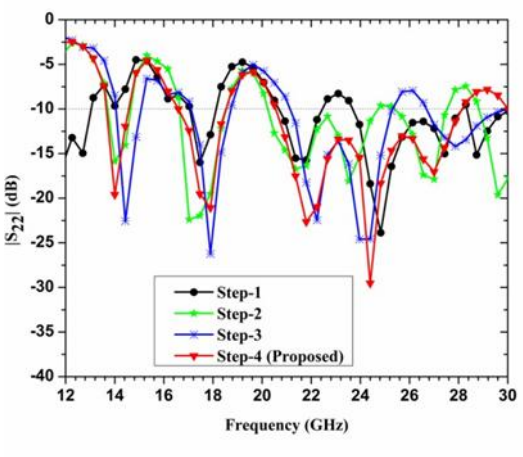

(b)

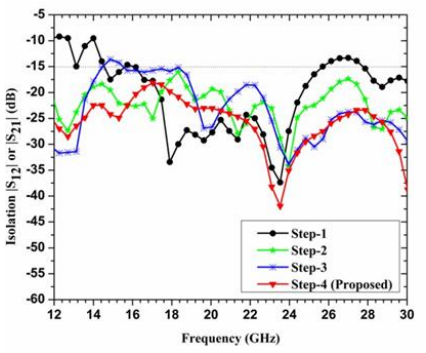

(c)

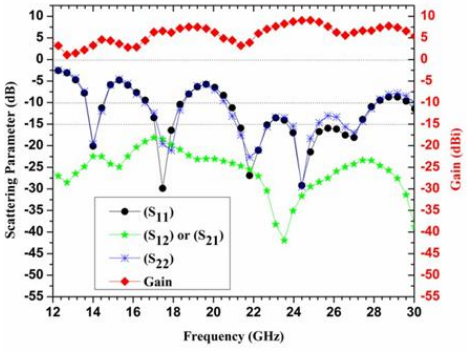

(d)

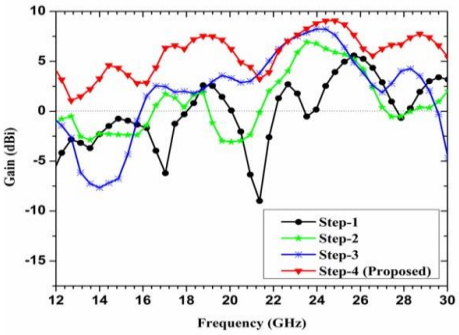

(e)

Fig. 3. Simulated performance of the antennas: (a) Return loss at port-1 (|S11|), (b) Return loss at port-2 (|S22|), (c) Port-to-port isolation (|S12| and |S21|), (d) Scattering parameters and gain of the proposed antenna (Step-4), and (e) Gain versus frequency comparison for all design steps (Step-1 to Step-4).

A comparative overview of the antennas from Step-1 to Step-4 is presented in Table 2, detailing their operating bands (GHz), bandwidths (GHz), port isolation (dB), resonant frequencies (GHz), reflection coefficients (dB), and peak gains (dBi) for both ports. The simulated S-parameters:|S11|, |S22|, |S12|, and |S21| for all steps are illustrated in Figure 3(a–c). The scattering parameters of the proposed antenna (Step-4) are explicitly shown in Figure 3(d), while Figure 3(e) compares the gain responses across all design steps. These results clearly demonstrate the progressive enhancements in antenna performance achieved through the systematic, step-wise design modifications, highlighting improvements in bandwidth, gain, and port isolation.

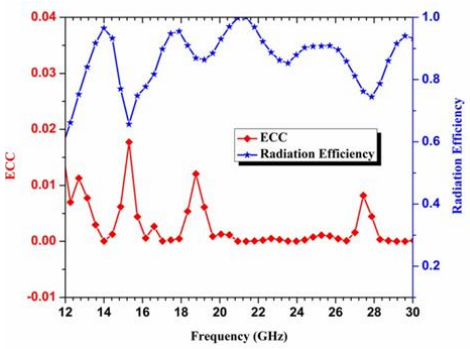

(a)

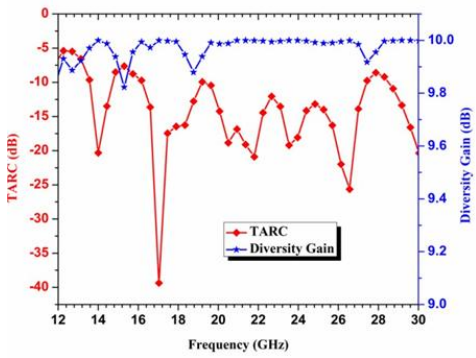

(b)

Fig. 4. Simulated MIMO performance of the proposed antenna (Step-4): (a) Envelope Correlation Coefficient (ECC) and Radiation Efficiency versus frequency, (b) Total Active Reflection Coefficient (TARC) and Diversity Gain (DG) versus frequency.

The proposed MIMO antenna exhibits multiple operating bands with consistent performance across both ports. For port-1, the antenna resonates at 14 GHz with a peak gain of 3.26 dBi within the 13.56–14.86 GHz band, at

17.46 GHz with 6.59 dBi in the 16.60–18.76 GHz band, and at 21.80, 24.40, and 27 GHz with peak gains of 3.89, 9.06, and 6.24 dBi, respectively, within the 20.50–28.36 GHz band (cf. Fig. 3 and Table 2). Similarly, for port-2, resonances occur at 14.10 GHz (3.26 dBi), 17.90 GHz (6.59 dBi), 21.86, 24.36, and 27.13 GHz (3.89, 9.06, and 6.24 dBi) within the same respective bands, showing negligible variation between the two ports due to the symmetrical MIMO configuration.

Table 2: Comparative performance analysis of MIMO antenna designs from antenna 1 to 4

Antenna	Port No.	Operating band (GHz)	Isolation (dB)	Resonant frequency (GHz)	Reflection Coefficients (dB)	Peak Gain (dBi)
Antenna-1	Port-1	13.56-14.43	≤ 10	14.00	-11.26	-2.3
		17.03-18.33	≤ 17	17.46	-16.85	-1.25
		20.50-22.23	≤ 24	21.36	-16.51	-8.98
		23.96-28.30	≤ 13	24.83	-22.46	3.92
				25.70	-22.29	5.58
	Port-2	17.03-18.33	≤ 17	17.46	-15.98	-1.25
		20.50-22.30	≤ 24	21.80	-15.73	-2.60
		23.96-28.30	≤ 13	24.83	-23.86	3.92
				27.43	-15.01	0.96
Antenna-2	Port-1	13.56-14.86	≤ 18	14.43	-15.62	-2.28
		16.60-18.76	≤ 16	17.03	-26.48	1.72
		20.06-22.23	≤ 19	20.93	-19.35	-2.36
		23.10-27.43	≤ 17	23.53	-16.23	6.92
				26.13	-16.28	4.2
	Port-2	13.56-14.86	≤ 18	14.00	-15.88	-2.26
		16.60-18.76	≤ 16	17.03	-22.40	1.72
		20.50-24.40	≤ 19	23.53	-18.08	6.92
		25.70-27.43	≤ 17	27.00	-17.88	0.38
Antenna-3	Port-1	14-15.30	≤ 13	14.43	-18.30	-7.19
		17.46-19.20	≤ 15	17.9	-22.92	2.00
		20.93-27.86	≤ 18	22.23	-25.61	6.24
				24.83	-28.43	7.65
	Port-2	14-15.30	≤ 13	14.43	-18.30	-7.19
		17.03-18.76	≤ 15	17.90	-22.92	2.00
		20.93-25.26	≤ 18	23.96	-24.59	8.21
		26.56-29.60	≤ 18	27.86	-14.19	4.01
Antenna-4	Port-1	13.56-14.86	≤ 22	14.00	-20.06	3.26
		16.60-18.76	≤ 18	17.46	-29.86	6.59
		20.50-28.36	≤ 23	21.80	-26.90	3.89
				24.40	-29.21	9.06
				27.00	-18.09	6.24
	Port-2	13.56-14.86	≤ 22	14.10	-19.60	3.26
		16.60-18.76	≤ 18	17.90	-21.07	6.23
		20.50-28.36	≤ 23	21.86	-22.66	3.89
				24.36	-29.54	9.06
				27.13	-17.03	6.24

The antenna achieves port isolation better than 18 dB, which is significantly higher than most reported designs, ensuring minimal mutual coupling and suitability for radar and satellite communication applications. The overall maximum and minimum peak gains are 9.06 dBi and 3.26 dBi at both ports, respectively. Table 2 summarizes the comprehensive performance of all antenna steps (Step-1 to Step-4), detailing the operating bands, bandwidths, port isolation, reflection coefficients, and peak gains, clearly illustrating the progressive improvement in performance through the step-wise design modifications. Step-wise comparison; table 2 provides a comprehensive comparison of the antennas developed from Step-1 to Step-4. Among these, the proposed antenna (Step-4) exhibits superior performance in terms of bandwidth, peak gain, and isolation for both ports. The analysis of Fig. 3 and Table 2 indicates that the operating frequency bands and gain characteristics are nearly identical at ports 1 and 2.

The negligible differences between the ports are attributed to the symmetrical placement of the radiating elements, which are separated by an optimized 2 mm spacing. This arrangement forms an effective MIMO configuration while maintaining a compact low-profile structure of 24×24×1.6 mm³, ensuring practical applicability in modern communication systems.

The diversity performance of the proposed dual-port rectangular patch MIMO antenna has been evaluated using HFSS simulations, focusing on Envelope Correlation Coefficient (ECC), Diversity Gain (DG), and Total Active Reflection Coefficient (TARC). These metrics are critical for assessing the antenna's MIMO capability, inter-element isolation, and overall system efficiency.
The ECC can be derived using either the radiation patterns or the scattering parameters of the antenna. As reported in [27], the measured and simulated ECC of the proposed antenna is computed by employing both the S-parameters and far-field radiation characteristics, as defined in Equations (1) and (2). The Envelope Correlation Coefficient (ρ or ECC) quantifies the correlation between the radiation patterns of multiple antenna elements. ECC ranges from 0 (completely uncorrelated) to 1 (fully correlated). A low ECC value signifies minimal mutual coupling and superior diversity performance. ECC can be derived either from the antenna's radiation patterns or its scattering parameters (S-parameters). For a 2-port MIMO system, ECC is computed from S-parameters as:

$$E_{CC}^{ij} = \frac{\left|S_{ii}^{*}S_{ij} + S_{ji}^{*}S_{jj}\right|^{2}}{\left(1 - |S_{ii}|^{2} - \left|S_{ji}\right|^{2}\right)\left(1 - \left|S_{jj}\right|^{2} - \left|S_{ij}\right|^{2}\right)} \quad (1)$$

$$ECC = \frac{|f_{4\pi}f_1(\theta,\phi)\cdot f_2(\theta,\phi)d\Omega|^{2}}{\int_{4\pi}|f_1(\theta,\phi)|^{2}d\Omega \cdot \int_{4\pi}|f_2(\theta,\phi)|^{2}d\Omega} \quad (2)$$

In this analysis, $f_1(\theta,\phi)$ represents the electric field component when element 1 is excited while element 2 is terminated with a matched load. Conversely, $f_2(\theta,\phi)$ denotes the electric field component when element 2 is excited and element 1 is terminated with the corresponding load.
For the proposed antenna, the simulated ECC remains below 0.012 across all operating bands (Figure 4(a)), which is far below the acceptable limit of 0.5. This confirms minimal mutual coupling between the ports and demonstrates effective diversity performance.

Diversity Gain (DG) evaluates the improvement in received signal quality provided by multiple antenna elements. It enhances the signal-to-noise ratio (SNR) without increasing input power, effectively mitigating multipath fading. DG is related to ECC and is calculated as (Equation 3):

$$\mathrm{DG} = 10\sqrt{1 - (ECC^{i,j})^{2}} \quad (3)$$

As illustrated in Figure 4(b), the DG for the proposed antenna exceeds 9.99 dB, closely approaching the ideal value of 10 dB. This confirms that the antenna maximizes received signal quality, supports stable wireless links, and exhibits excellent diversity characteristics across all operating bands.

TARC for a dual-port configuration can be determined its detailed formulation for multi- port systems is expressed by equation (4), as reported in [11–24]. A lower TARC signifies enhanced impedance matching, improved isolation, and better diversity characteristics, ultimately leading to higher efficiency and superior MIMO performance TARC evaluates the overall reflection behavior of a MIMO antenna under simultaneous multi-port excitation. It indicates how the excitation of one antenna element affects the performance of other elements. For a 2-port system, TARC is expressed as:

$$\mathrm{TARC} = \frac{\sqrt{\left|\sum_{i=1}^{N} S_{i1} + \sum_{m=2}^{N} S_{im}e^{j\theta_{m-1}}\right|}}{\sqrt{N}} \quad (4)$$

Lower TARC values indicate improved impedance matching, enhanced isolation, and better diversity performance. For the proposed antenna, TARC remains below –10 dB across all operating bands (Figure 4(b)), demonstrating excellent multi-port impedance matching and minimal reflected power under simultaneous excitation of both ports.

The simulated radiation efficiency of the proposed dual-port MIMO antenna remains above 85% across all resonant frequency bands (Figure 4(a)), indicating that the antenna effectively converts input power into radiated

energy. This high efficiency demonstrates the antenna's suitability for practical multi-band applications, including Ku- and K-band radar, satellite, and vehicular communication systems, while minimizing power losses and maintaining robust performance.

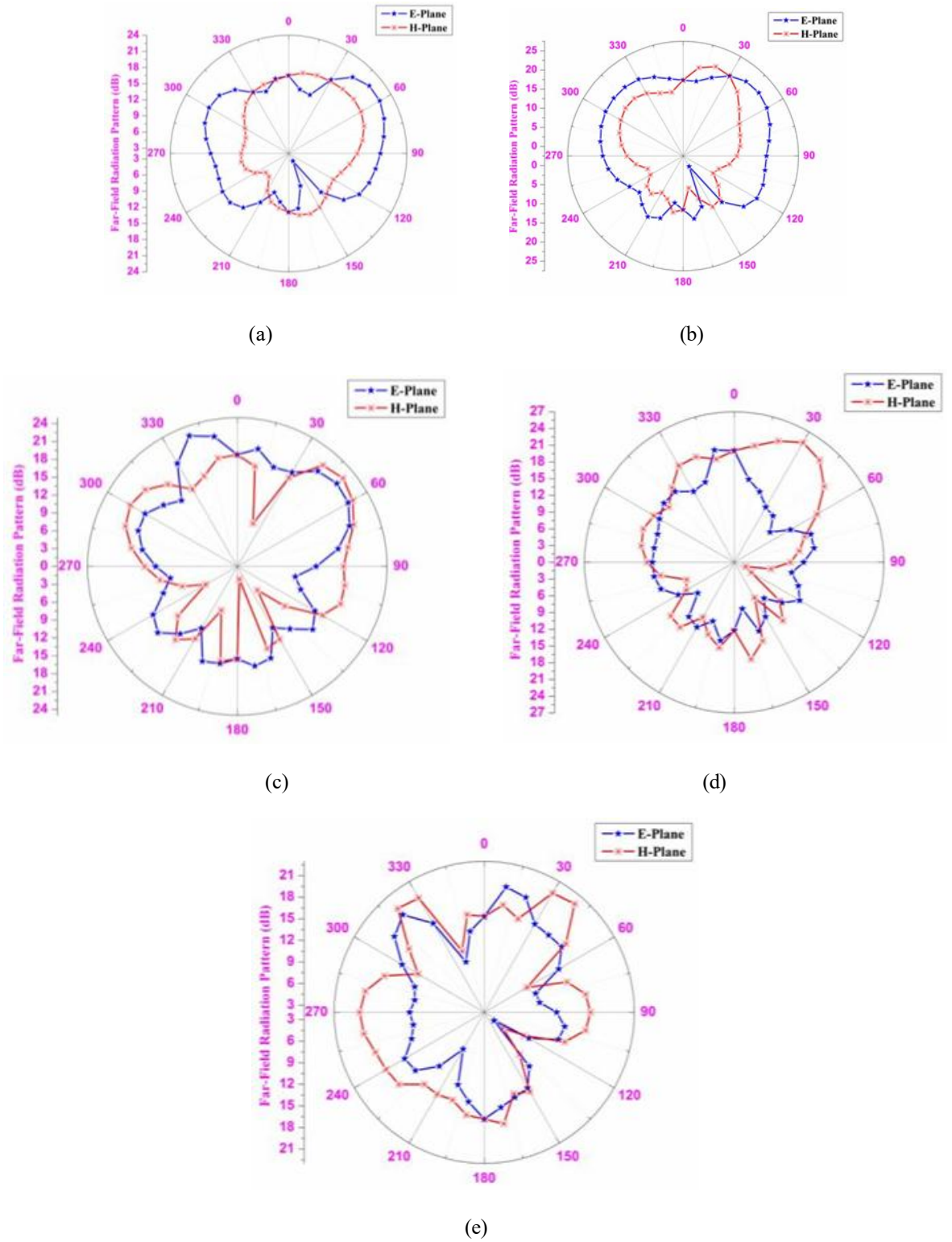

Fig. 5. Simulated far-field radiation patterns of the proposed antenna (Step-4) at port-1 in the E-plane and H-plane: (a) 14 GHz, (b) 17.46 GHz, (c) 21.80 GHz, (d) 24.40 GHz, and (e) 27 GHz.

The far-field radiation patterns of the proposed antenna were simulated for both co-polarization and cross-polarization in the E-plane and H-plane, with the elevation axis corresponding to the polar axis (φ = 0°). The

antenna's radiation was analyzed at 14 GHz, 17.46 GHz, 21.80 GHz, 24.40 GHz, and 27 GHz, as shown in Figure 5(a-e) for port-1. The results indicate that the proposed antenna exhibits broad omnidirectional radiation patterns across all operating frequencies, which is ideal for vehicular, radar, and satellite communication applications. The consistent and uniform radiation characteristics confirm the suitability of the design for multi-frequency MIMO operations, ensuring robust performance in practical communication systems.

4. Comparative Analysis with Modern Literature

The proposed dual-port MIMO antenna (Step-4) is evaluated against several reported MIMO antennas in terms of antenna size, number of ports, operating band, peak gain, envelope correlation coefficient (ECC), diversity gain (DG), isolation, total active reflection coefficient (TARC), and radiation efficiency (RE). The detailed comparison is presented in Table 3**.**

Table 3: A comparative overview of the proposed MIMO antenna with reported antenna

Ref.	Antenna Size (mm^3)	No. of Ports	Operating Band	Peak Gain (dBi)	ECC	DG (dB)	Isolation (dB)	TARC (dB)	RE (%)
[21]	42×85×0.58	2	27–32	7.9	NR	NR	-17.1	NR	70
[22]	48×21×0.13	2	29.5–31.5	7.1	0.002	9.9	-26	NR	NR
[23]	30×30×0.0009	4	27.5–29.5	5.8	0.03	10	-26	NR	80
[24]	55×50×1.6	2	15.31–20.02 25.6–35.21	7.5	0.005	9.9	-20	<0	NR
[25]	30×52×1.6	2	2–3.6 6.6–7.9 9.6–12.7 11–15.6	5–6.6	0.024	9.9	-20	<-9.96	NR
[26]	30×30×1.6	2	24.95–31.31	8.2	0.0012	9.9	-15	NR	70
[27]	32×20×0.8	2	3.3–7.8 8–12	3	0.05	9.8	-20	<10	69
[28]	30×30×1.6	2	10–15	6.8	0.01	9.7	-18	-12	72
[29]	35×35×1.2	2	12–18	7.4	0.02	9.6	-19	-11	74
[30]	28×28×1.0	2	14–28	8.5	0.015	9.9	-21	-10	78
Proposed	24×24×1.6	2	13.56–14.86 16.60–18.76 20.50–28.36	3.26–9.06	0.012	9.9	-18 to -23	< -10	85

From the comparison, it is evident that the proposed antenna is the most compact design (24×24×1.6 mm^3) among all reported antennas. Despite its smaller size, it supports multi-band operation covering 13.56–14.86 GHz, 16.60–18.76 GHz, and 20.50–28.36 GHz, which is wider than many previous designs. The peak gain varies from 3.26 to 9.06 dBi, demonstrating good radiation performance across all operating bands.

The envelope correlation coefficient (ECC) of the proposed antenna is only 0.012, indicating excellent diversity performance, while the diversity gains (DG) is maintained at 9.9 dB, comparable with the best reported designs. The isolation between the two ports ranges from -18 dB to -23 dB, which ensures minimal mutual coupling, and the TARC remains below -10 dB for all bands, confirming efficient reflection characteristics. Additionally, the radiation efficiency (RE) reaches 85%, surpassing most of the antennas listed in literature [21-30].

Overall, the proposed antenna demonstrates superior performance in compactness, multi-band operation, gain, isolation, ECC, DG, TARC, and efficiency, making it highly suitable for modern vehicular, satellite, and radar communication applications.

5. Conclusions

In this work, a compact dual-port MIMO antenna with overall dimensions of 24×24×1.6 mm^3 has been successfully designed and analyzed for Ku and K-band radar and satellite communication applications. The antenna comprises two identical radiating elements arranged in parallel to maximize inter-element isolation and minimize mutual coupling. The design is implemented on an FR-4 epoxy substrate ($\varepsilon_r = 4.4$, $\tan\delta = 0.02$, thickness h = 1.6 mm) and thoroughly simulated using HFSS. The simulation results indicate that the proposed antenna achieves a peak gain ranging from 3.26 dBi to 9.06 dBi across the operating bands, with maximum and minimum gains of 9.06 dBi and 3.26 dBi, respectively. The Diversity Gain (DG) remains close to the ideal 10 dB (9.99–10 dB), the Total Active Reflection Coefficient (TARC) stays below -10 dB, and the radiation efficiency exceeds

85%, confirming high-performance operation across all targeted frequencies. The antenna demonstrates consistent performance at both ports, with simulated isolation ≤ -18 dB and an Envelope Correlation Coefficient (ECC) less than 0.012, indicating excellent diversity characteristics and minimal mutual coupling. Furthermore, the antenna exhibits omnidirectional radiation patterns, making it highly suitable for vehicular, radar, and satellite communication systems.

Overall, the proposed MIMO design offers a compact, efficient, and reliable multi-band solution, combining high gain, low ECC, strong isolation, and broad radiation efficiency, making it a promising candidate for advanced communication applications.

References

[1] M. Srinubabu, "A compact and efficiently designed two-port MIMO antenna," *International Journal of Engineering Research and Technology*, vol. 13, no. 2, pp. 201–206, 2024.

[2] A. Omrani and M. A. Abdalla, "An ultra-wideband microstrip MIMO antenna with EBG loading for WLAN and Sub-6G applications," *arXiv preprint arXiv:2303.08715*, Mar. 2023.

[3] S. Ismam, D. Hossain, S. M. Salam, and M. M. Rashid, "Design and performance analysis of 28 GHz two-port MIMO rectangular microstrip patch antenna array for 5G applications," *Asian Journal of Electrical and Electronic Engineering*, vol. 2, no. 3, pp. 45–52, Sept. 2023.

[4] M. A. Rahman, S. Islam, and T. K. Hoque, "Miniaturized dual-port multiband MIMO antenna with CSRR for wireless applications," *Wireless Communications and Mobile Computing*, vol. 2023, Art. ID 5568724, Apr. 2023.

[5] Kim-Thi, N. H. Nguyen, and T. T. Vu, "Compact and high-isolated dual-port microstrip patch antenna for 5G applications," *Procedia Computer Science*, vol. 230, pp. 921–928, 2024.

[6] S. Mohapatra, P. K. Mishra, and S. K. Behera, "Dual-band orthogonal polarized two-port MIMO antenna for LTE/C/X-band applications," *AEM Journal*, vol. 13, no. 1, pp. 54–62, 2024.

[7] S. Kamal, N. Singh, and V. Kumar, "Design and system performance analysis of a two-port MIMO antenna for LTE systems," *AIP Conference Proceedings*, vol. 2762, no. 1, pp. 020001, 2023.

[8] U. Sharma and R. K. Raj, "Quad-band dual-port MIMO microstrip antenna with double-stub structure for wireless applications," *Physica Scripta*, vol. 99, no. 2, Art. ID 025004, 2024.

[9] Din, I., "High Performance Antenna System in MIMO Configuration for Remote Sensing Applications," *AGU Publications*, 2023.

[10] Din, I. U., "A Novel and Compact Metamaterial-Based Four-Element MIMO Antenna for 5G mm-Wave Communication," *Hindawi*, 2024.

[11] Anouar, E., "Design aspects of MIMO antennas and its applications," *ScienceDirect*, 2024.

[12] Raj, T., "Advances in MIMO Antenna Design for 5G," *Sensors*, 2023.

[13] Elsharkawy, R. R., "A Compact Super-Wideband MIMO Antenna for Wireless Communication," *Progress In Electromagnetics Research C*, 2024.

[14] Jemaludin, N. H., et al., "A comprehensive review on MIMO antennas for 5G smartphones," *Science Progress*, 2024.

[15] Ali, A., et al., "A Compact MIMO Multiband Antenna for 5G/WLAN/WIFI-6 Applications," *Micromachines*, Vol. 14, No. 6, 1153, 2023.

[16] Salehi, M., and H. Oraizi, "Wideband High Gain Metasurface-Based 4T4R MIMO antenna with Highly Isolated Ports for Sub-6 GHz 5G Applications," *arXiv preprint*, 2023.

[17] Pandey, A., A. K. Singh, S. Singh, and R. Singh, "A compact Ultra-Wideband (UWB) MIMO antenna for K and Ka band applications," *IOT with Smart Systems*, 117-126, Springer, Singapore, 2022.

[18] Urimubenshi, F., D. B. Konditi, J. de Dieu Iyakaremye, P. M. Mpele, and A. Munyaneza, "A novel approach for low mutual coupling and ultra-compact two port MIMO antenna development for UWB wireless application," *Heliyon*, Vol. 8, No. 3, e09057, 2022.

[19] Bhatia, S. S. and N. Sharma, "Modified spokes wheel shaped MIMO antenna system for multiband and future 5G applications: Design and measurement," *Progress In Electromagnetics Research C*, Vol. 117, 261-276, 2021.

[20] Dwivedi, A. K., A. Sharma, A. K. Singh, and V. Singh, "Meta-material inspired dielectric resonator MIMO antenna for isolation enhancement and linear to circular polarization of waves," *Measurement*, Vol. 182, 109-681, 2021.

[21] Murali Krishna, C., M. Sai Prapoorna, K. Taruni Sesha Sai, and M. Sai Teja, "Super wideband MIMO antenna for advanced wireless communication," *Advances in Electrical and Computer Technologies*, 509-519, Springer, Singapore, 2021.

[22] Saxena, G., P. Jain, and Y. K. Awasthi, "High diversity gain super-wideband single band-notch MIMO antenna for multiple wireless applications," *IET Microwaves, Antennas & Propagation*, Vol. 14, No. 1, 109-119, 2020.

[23] Rahman, S., X. C. Ren, A. Altaf, M. Irfan, M. Abdullah, F. Muhammad, and F. S. AlKahtani, “Nature inspired MIMO antenna system for future mm-Wave technologies," *Micromachines*, Vol. 11, No. 12, 1083, 2020.
[24] Sehrai, D. A., M. Abdullah, A. Altaf, S. H. Kiani, F. Muhammad, M. Tufail, and S. Rahman, “A novel high gain wideband MIMO antenna for 5G millimeter wave applications," *Electronics*, Vol. 9, No. 6, 1031, 2020.
[25] Addepalli, T. and V. R. Anitha, “Compact two-port MIMO antenna with high isolation using parasitic reflectors for UWB, X and Ku band applications," *Progress In Electromagnetics Research C*, Vol. 102, 63-77, 2020.
[26] Dwivedi, A. K., A. Sharma, A. K. Singh, and V. Singh, “Circularly polarized quad-port MIMO dielectric resonator antenna with beam tilting feature for vehicular communication," *IETE Technical Review*, 1-13, 2020.
[27] Tan, C. M. and M. R. Tripathy, “A miniaturized T-shaped MIMO antenna for X-band and Ku-band applications with enhanced radiation efficiency," *2018 27th Wireless and Optical Communication Conference (WOCC)*, 1-5, IEEE, April 2018.
[28] Pouyanfar, N., C. Ghobadi, J. Nourinia, K. Pedram, and M. Majidzadeh, “A compact multi-band MIMO antenna with high isolation for C and X bands using defected ground structure," *Radio Engineering*, Vol. 27, No. 3, 686-693, 2018.
[29] Chilukuri, S., K. Dahal, and A. Lokam, “Multi-port pattern diversity antenna for K and Ka-band application," *Advanced Electromagnetics*, Vol. 7, No. 2, 5-9, 2018.
[30] Sharawi, M. S., S. K. Podilchak, M. T. Hussain, and Y. M. Antar, “Dielectric resonator based MIMO antenna system enabling millimetre-wave mobile devices," *IET Microwaves, Antennas & Propagation*, Vol. 11, No. 2, 287-293, 2017.
[31] Jilani, S. F. and A. Alomainy, “A multiband millimeter-wave 2-D array based on enhanced Franklin antenna for 5G wireless systems," *IEEE Antennas and Wireless Propagation Letters*, Vol. 16, 2983-2986, 2017.
[32] Hussain, R., A. T. Alreshaid, S. K. Podilchak, and M. S. Sharawi, “Compact 4G MIMO antenna integrated with a 5G array for current and future mobile handsets," *IET Microwaves, Antennas & Propagation*, Vol. 11, No. 2, 271-279, 2017.
[33] Rappaport, T. S., Y. Xing, G. R. MacCartney, A. F. Molisch, E. Mellios, and J. Zhang, “Overview of millimeter wave communications for fifth-generation (5G) wireless networks with a focus on propagation models," *IEEE Transactions on Antennas and Propagation*, Vol. 65, No. 12, 6213-6230, 2017.
[34] Li, Y., C. Wang, H. Yuan, N. Liu, H. Zhao, and X. Li, “A 5G MIMO antenna manufactured by 3-D printing method," *IEEE Antennas and Wireless Propagation Letters*, Vol. 16, 657-660, 2016.
[35] Park, J. S., J. B. Ko, H. K. Kwon, B. S. Kang, B. Park, and D. Kim, “A tilted combined beam antenna for 5G communications using a 28-GHz band," *IEEE Antennas and Wireless Propagation Letters*, Vol. 15, 1685-1688, 2016.
[36] Wang, C. X., F. Haider, X. Gao, X. H. You, Y. Yang, D. Yuan, and E. Hepsaydir, “Cellular architecture and key technologies for 5G wireless communication networks," *IEEE Communications Magazine*, Vol. 52, No. 2, 122-130, 2014.
[37] Wu, D., S. W. Cheung, T. I. Yuk, and X. L. Sun, “A planar MIMO antenna for mobile phones," *PIERS Proceedings*, 1150-1152, Taipei, March 25-28, 2013.
[38] Rahimian, A. and F. Mehran, “RF link budget analysis in urban propagation microcell environment for mobile radio communication systems link planning," *2011 International Conference on Wireless Communications and Signal Processing (WCSP)*, 1-5, IEEE, November 2011.
[39] Chiu, C. Y., C. H. Cheng, R. D. Murch, and C. R. Rowell, “Reduction of mutual coupling between closely-packed antenna elements," *IEEE Transactions on Antennas and Propagation*, Vol. 55, No. 6, 1732-1738, 2007.
[40] Alhalabi, R. A. and G. M. Rebeiz, “High-efficiency angled-dipole antennas for millimeter-wave phased array applications," *IEEE Transactions on Antennas and Propagation*, Vol. 56, No. 10, 3136-3142, 2008.